Journal of Power Sources 195 (2010) 3119–3123

Contents lists available at ScienceDirect

Journal of Power Sources

journal homepage: www.elsevier.com/locate/jpowsour

Short communication

Cu–YSZ cermet solid oxide fuel cell anode prepared by high-temperature sintering

Michael C. Tucker*, Grace Y. Lau, Craig P. Jacobson, Steven J. Visco, Lutgard C. De Jonghe

Materials Sciences Division, Lawrence Berkeley National Laboratory, 1 Cyclotron Rd., MS 62-203, Berkeley, CA 94720, USA

ARTICLE INFO

Article history:
Received 27 October 2009
Received in revised form 1 December 2009
Accepted 1 December 2009
Available online 4 December 2009

Keywords:
SOFC
YSZ
Cermet
Copper

ABSTRACT

Porous YSZ–Cu alloy cermet structures are prepared by sintering above the metal melting point in reducing atmosphere. Unexpectedly good wetting of the molten metal within the YSZ network is obtained, resulting in cermets with fine structure and excellent electronic conductivity. Anode-supported solid oxide fuel cells are prepared with YSZ–Cu alloy cermet as the anode. Addition of infiltrated ceria catalyst improved the initial performance. Maximum power density of about 275 mA cm^{-2} and operation for about 110 h was achieved in the 700–800 °C range. After operation, AC impedance revealed that the high-frequency impedance was unchanged, whereas the low-frequency impedance increased. It was concluded that the Cu alloy network conductivity remains high, but catalyst stability needs improvement.

1. Introduction

State-of-the-art solid oxide fuel cell (SOFC) anodes are typically formed from Ni–YSZ cermets. This cermet consists of interpenetrating, well-connected networks of Ni and YSZ that provide electronic and ionic conduction through the electrode. In a thin region near the anode–electrolyte interface, the Ni acts as catalyst for the fuel oxidation reaction. The Ni–YSZ anode has been most widely developed because of its ease of manufacture, performance, and longevity. Disadvantages of using Ni as the anode catalyst and electronic conductor include redox instability, susceptibility to coking by hydrocarbon fuel, and poisoning by fuel impurities such as sulfur [1]. As such, many alternative anode compositions are under investigation.

Replacing Ni with Cu has the potential to greatly enhance anode tolerance to dry hydrocarbons, thereby eliminating coking and thus enabling internal reforming [2]. The Cu/Cu-oxide transition occurs at higher oxygen partial pressure than the Ni/Ni-oxide transition, so improved redox tolerance is expected as well. Furthermore, the price of Cu has historically been only 25–50% the price of Ni [3]. Unfortunately, the production of Cu–YSZ structures is not as straightforward as for Ni–YSZ. Ni–YSZ cermets are typically created by sintering a mixture of Ni-oxide and YSZ in air at high temperature (1200–1450 °C). The Ni-oxide is then converted to metallic Ni upon exposure to reducing atmosphere at elevated temperature (400–1000 °C). The fuel stream of an SOFC is suitably reducing to effect this transition. In contrast, Cu and copper oxide melt below 1200 °C. Molten metals do not generally wet ceramic surfaces, so the temperature of cermet preparation is typically below the melting point of the metal, or else the metal will dewet, pool, or extrude from the ceramic network. Thus, it is generally accepted that Cu–YSZ cermet cannot be processed by the powder sintering methods applied to Ni–YSZ.

An alternative fabrication approach for Cu–YSZ anode structures has been developed, most notably by Gorte and Vohs [1,4,5]. Porous YSZ layers are fabricated at high temperature, followed by impregnation of Cu and CeO_2 precursor solutions at low temperature. The infiltration process must be repeated many times to build up sufficient Cu loading such that an efficient percolating network for electron transport is provided. The result is a YSZ backbone coated with a continuous, porous blanket of sub-micrometer Cu and CeO_2 particles. Such electrodes have shown good performance and stability, even with direct methane fuel feed and high sulfur content [1]. Unfortunately, because of the small Cu and CeO_2 particle size, coarsening leads to loss of performance at temperatures above 700 °C. Cu–YSZ nanocomposites have also been prepared by wet chemical routes, but the zirconia particles are not well-sintered enough to expect ionic conductivity through the structure.[6]

It is desirable to fabricate Cu–YSZ anode cermets in a single step at high temperature (>1200 °C), thus quickly producing a coarse structure that is expected to be stable at the lower fuel cell operating temperature (500–900 °C). In this work, we report preparation and performance of a YSZ–Cu alloy cermet anode fabricated by firing a mixture of YSZ and Cu powder at high temperature in reducing atmosphere. Copper oxide reacts with YSZ at 1200 °C and above, so we have explored the use of reducing atmosphere sintering such

* Corresponding author. Tel.: +1 510 486 5304; fax: +1 510 486 4881.
E-mail address: mctucker@lbl.gov (M.C. Tucker).

0378-7753/$ – see front matter © 2009 Elsevier B.V. All rights reserved.
doi:10.1016/j.jpowsour.2009.12.003

that Cu is in the reduced metal state and does not react significantly with YSZ. Of course, the copper is molten (melting point 1083 °C) so wetting on YSZ is of primary concern. Some guidance for improving wetting of molten copper on YSZ is available in the literature. Zr–Cu alloys successfully wet stabilized zirconia [7]. The best wetting was observed for Zr–Cu (63–37 wt%). Unfortunately, the high Zr content required to promote wetting suggests that the alloy will readily oxidize in the SOFC fuel atmosphere with a concomitant volume expansion and reduction in electrical conductivity expected. Addition of Cr and Ni was also shown to improve wetting of molten Cu on a ZrO_2 plate [8]. True wetting (contact angles below 90°) was observed for small additions of Ni and Cr and temperatures between 1150 and 1350 °C. Based on these results, we have used a 96Cu–4Ni–1Cr (wt) alloy composition throughout this work.

2. Experimental details

2.1. Bulk sample preparation

A mixture of 5 g 8Y YSZ (Tosoh Corp), 4.75 g Cu, 0.2 g Ni, 0.073 g Cr_2O_3 (all powder particle sizes 1.5 μm or less), and 0.2 g HPC (hydroxypropylcellulose) was ball milled 24 h in IPA (isopropyl alcohol). The mixture was then dried, ground and sieved to <150 μm. The resulting powder was uniaxially pressed into 0.5 in. diameter pellets at 10 kpsi. Pellets were fired at 1100–1300 °C in reducing atmosphere (4% H_2, balance Ar) for 2 h.

2.2. Electrochemical cell preparation

Planar cell: A mixture of 5 g 8Y YSZ (Tosoh Corp), 4.75 g Cu, 0.2 g Ni, 0.073 g Cr_2O_3 (all powder particle sizes 1.5 μm or less), 0.12 g PMMA (polymethylmethacrylate) poreformer (0.5–11 μm particle size), and 0.2 g HPC (hydroxypropylcellulose) was ball-milled 24 h in IPA (isopropyl alcohol). The mixture was then dried, ground and sieved to <150 μm. The resulting powder was uniaxially pressed into 1 in. diameter disks at 10 kpsi. A disk was bisque fired at 1000 °C in reducing atmosphere (4% H_2, balance Ar) for 2 h. One side of the disk was then aerosol sprayed with a thin layer of 8Y YSZ from a solution of IPA and DBT (dibutylphthalate) dispersant. The resulting bilayer was cosintered in reducing atmosphere at 1300 °C for 4 h. After sintering, the YSZ/Cu alloy support layer was electronically conductive at room temperature, and the thin YSZ electrolyte film was dense with no cracks or pinholes. An LSCF cathode was deposited by aerosol spray to the electrolyte surface. Electrical leads consisting of Pt paste and Pt mesh were applied to the LSCF cathode and YSZ/Cu alloy support. The complete cell was mounted on a test rig and heated to 800 °C for fuel cell testing with ambient air on the cathode side and moist hydrogen flowing to the anode side.

Tubular cell: A tubular cell was prepared as described above. The YSZ–Cu alloy tube was prepared by cold isostatic press. After cosintering with the electrolyte layer, the infiltrated LSM–YSZ cathode was added and the complete cell was brazed to a stainless steel housing, as described elsewhere [9,10].

2.3. Sample characterization

SEM/EDS analysis was obtained with a Hitachi S-4300SE/N scanning electron microscope in secondary electron imaging mode. Smooth cross-sections were obtained using a dual focused ion and electron beam (FIB/SEM; FEI Strata 235M) system.

2.4. Cell testing and analysis

Polarization curves were obtained using LabView software controlling a power supply (Kepco). AC impedance spectra were obtained with a potentiostat/frequency response analyzer (Solartron 1286/1255) in frequency sweep mode from 10^6 to 0.1 Hz. Fuel was hydrogen passed through a water bubbler at room temperature.

3. Results and discussion

3.1. Preparation of YSZ–Cu alloy cermet pellets

Fig. 1 shows the microstructure of YSZ–Cu alloy cermet pellets after sintering at various temperatures in reducing atmosphere. At 1100 °C, we assume the Cu alloy is just above its melting point (pure copper melts at 1083 °C, and addition of Ni increases the melting point, but small additions of Cr decrease the melting point). The molten Cu alloy occupies the void space within the porous YSZ lat-

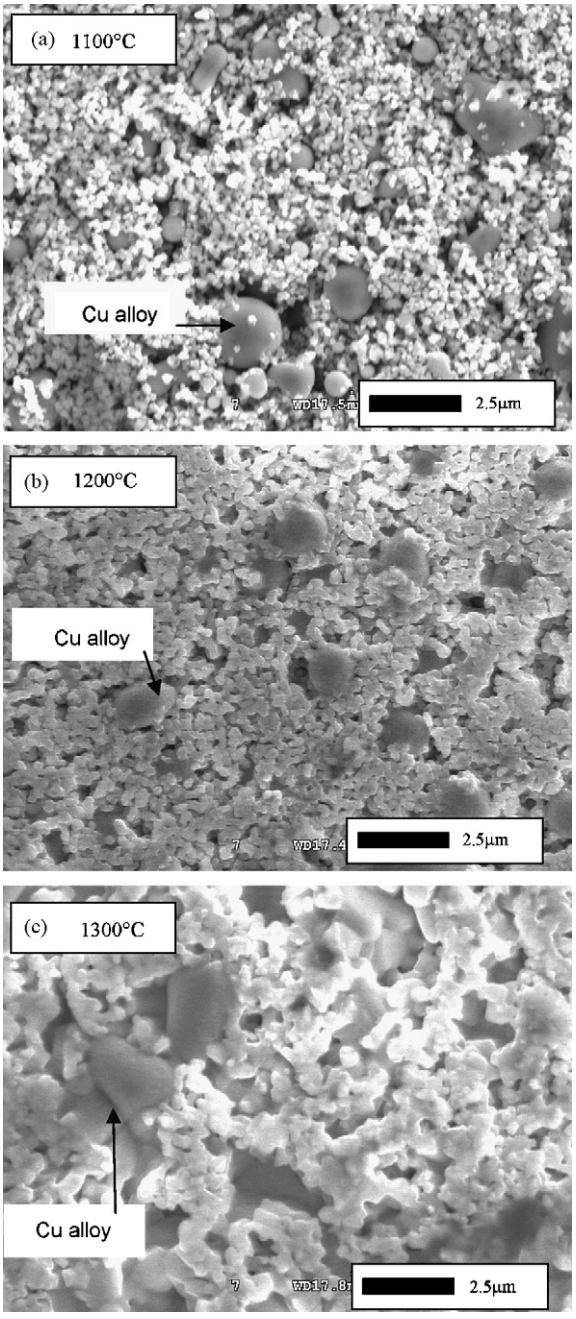

Fig. 1. SEM images of the surface of YSZ–Cu alloy cermet pellets after firing to various temperatures in reducing atmosphere (4% H_2/96% Ar).

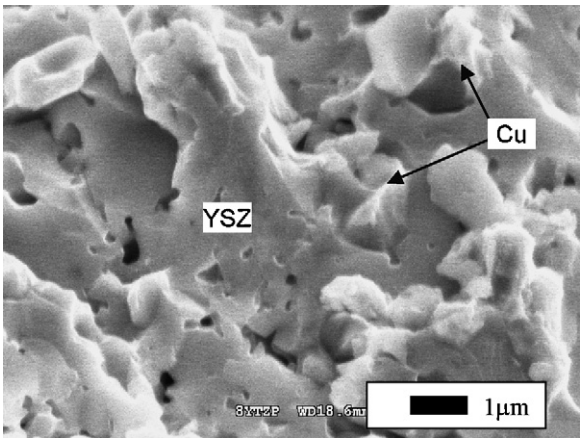

Fig. 2. SEM image of fracture surface of YSZ-Cu alloy cermet pellet after firing to 1300 °C in reducing atmosphere.

tice. Isolated spheres of Cu alloy are observed due to non-wetting interaction between the molten alloy and YSZ network, and the structural integrity of the cermet is largely dictated by the YSZ phase at this point. As expected, there is no noticeable YSZ sintering at this temperature. At 1200 °C, the YSZ particles have begun to sinter, forming a well-connected network. The Cu alloy particles are less spherical, and appear to wet the YSZ to some extent. The Cu alloy remains as largely isolated particles at this temperature; no electrical conductivity through the sample was detected after cooling to room temperature. Dramatically different morphology is observed after sintering to 1300 °C. A fracture surface of the same specimen is shown in Fig. 2. Ductile failure is observed in the Cu alloy phase. The YSZ network is sintered well, and the Cu alloy wets the YSZ surface unexpectedly well. Because of this wetting, the Cu alloy particles spread over the YSZ surface enough to contact each other, resulting in a well-connected Cu alloy network. The sample was highly electrically conductive after cooling to room temperature. The features of the Cu alloy network remain small (1–10 μm), in contrast to the bulk pooling and extrusion expected for a non-wetting molten metal in a porous framework. High-magnification EDAX was used to look for evidence of isolated Ni or Cr particles in the alloy phase. None were observed, suggesting complete alloying after firing at 1300 °C.

The exact nature of this transition to wetting behavior around 1300 °C is not clear. We presume, however, that it is related to reduction of the YSZ surface by the hydrogen-containing process

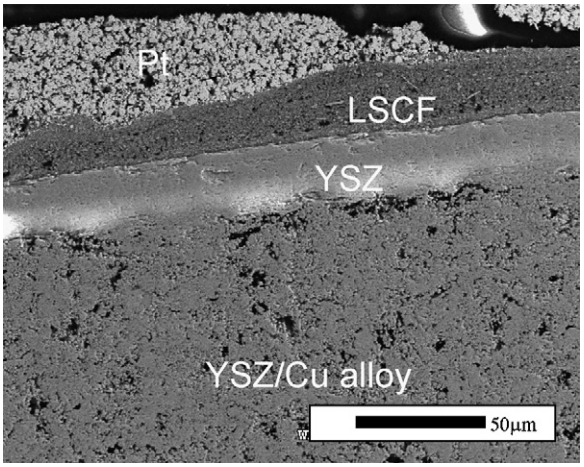

Fig. 3. SEM image of polished cross-section of planar YSZ–Cu alloy anode-supported cell after testing.

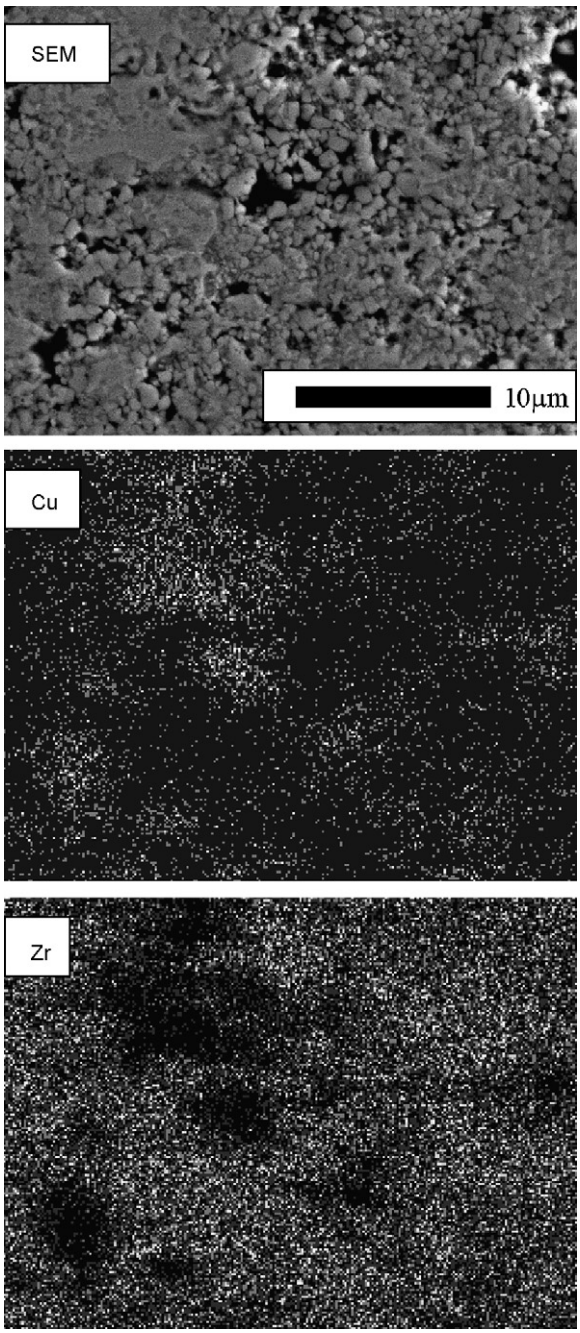

Fig. 4. Higher magnification SEM image of the YSZ–Cu alloy layer shown in Fig. 3, with Cu and Zr EDAX maps at the same magnification.

atmosphere. As the sintering temperature increases, the YSZ surface becomes reduced. This promotes wetting of the molten Cu alloy on the YSZ surface. Thus, pooling or complete extrusion of the molten metal (as would be expected if the alloy did not wet YSZ) is prevented. Instead, the molten alloy retains fine structure and remains as an interconnected lattice interpenetrating the YSZ lattice. This situation is analogous to the reactive element effect used in Ag–Cu alloy brazing to ceramic surfaces [9], although in this case reduction of the ceramic surface is achieved by hydrogen-containing atmosphere rather than addition of Ti or other easily oxidized metals. YSZ is expected to be more reduced at higher temperature for a given hydrogen-containing atmosphere, consistent with these results. It is therefore tempting to increase the sintering temperature above 1300 °C to further improve wetting. The vapor

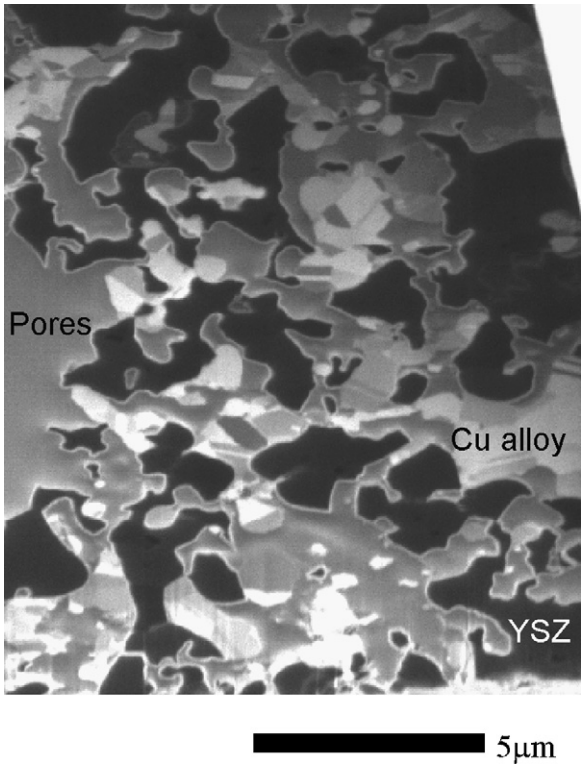

Fig. 5. Ion beam image of FIB-cut cross section of YSZ–Cu alloy layer shown in Fig. 3. YSZ appears dark, Cu alloy appears white, and epoxy-filled pores appear light gray.

pressure of Cu becomes significant at such high temperatures, however, so evaporation becomes a concern [11].

3.2. Performance of YSZ–Cu alloy anode-supported cells

As mentioned above, the Cu alloy is molten in the temperature region where YSZ sintering occurs (1100–1300 °C). Thus, the cermet sintering curve is largely dictated by the YSZ network, and very similar to pure YSZ. Cosintering a thin YSZ electrolyte layer with thicker YSZ–Cu alloy anode support is therefore straightforward. Planar anode-supported cells were easily prepared with minimal curvature. Figs. 3–5 show a cross section of one such cell after testing. Adequate bonding between the support and electrolyte is achieved. The fine structure of the YSZ and Cu phases is retained after firing and testing. Necking between YSZ particles is not as developed as is typically observed in YSZ-only structures. The SEM and EDS maps in Fig. 4 confirm that Cu alloy and YSZ are evenly distributed throughout the cermet support structure. The high magnification images show some regions of Cu alloy pooling into larger features, up to 10 μm in size. We presume that some of the Cu alloy extrudes into the pores introduced by the poreformer, which has an average particle size of 10 μm. Fig. 5 shows a focused ion beam (FIB)-cut cross-sectional surface of the anode; the image was produced with an ion beam rather than electron beam. This provides much better contrast between YSZ and Cu alloy. The dark areas are YSZ, the light gray areas are epoxy, and the white areas are Cu alloy. It is clear that the Cu alloy retains a very fine feature size.

The YSZ/Cu alloy cermet-supported cell with sprayed LSCF cathode was tested for electrochemical function. Fig. 6a shows AC impedance data for the full cell taken at 800 °C. The high-frequency impedance is quite good, indicating high electronic conductivity in the alloy phase. The total cell impedance probably contains a significant contribution from the LSCF cathode. Fig. 6b shows polarization

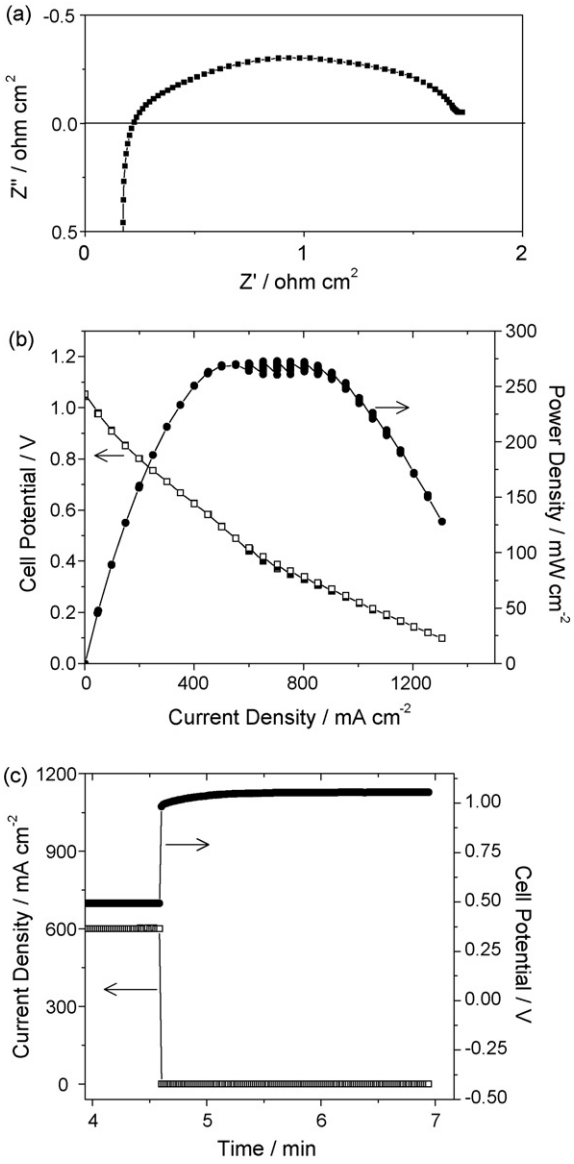

Fig. 6. Electrochemical performance of the planar YSZ/Cu alloy-supported cell shown in Fig. 3. All data obtained at 800 °C with air and 97% H_2/3% H_2O fuel. (a) Full cell AC impedance, (b) polarization, and (c) current interrupt.

behavior for the cell. The open circuit potential (OCP) is above 1.0 V, indicating good sealing and a leak-free electrolyte layer. Maximum power density is about 275 mW cm^{-2}. Rapid cell potential recovery after current interruption, shown in Fig. 6c, indicates that that ohmic and activation overpotentials are much larger than concentration polarization. Mass transport is adequate in the YSZ/Cu alloy and LSCF structures.

Tubular cells were also prepared with YSZ–Cu alloy as the support. A cell was braze-sealed to a stainless steel manifold and the cathode consisted of a porous YSZ backbone, infiltrated LSM catalyst, and porous stainless steel current collector, as described elsewhere [10,12]. Fig. 7a shows impedance for the cell before and after operation. The high-frequency impedance is quite small, indicating good electrical conductivity in the Cu alloy and infiltrated LSM phases. The total impedance is dominated by electrode polarization, presumably due to the relatively poor catalysis of the Cu alloy. The catalysis might be improved by adding more Ni to the alloy. The cell was cooled and fine ceria was added to the anode by infiltration, as described elsewhere [13]. Dramatic improve-

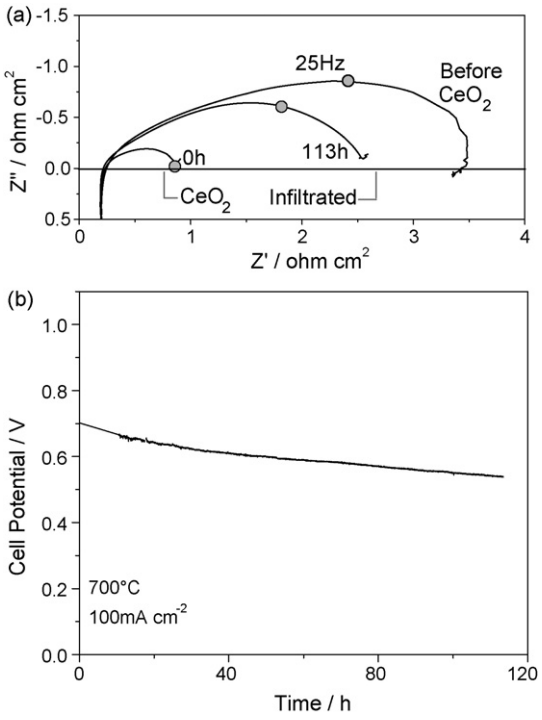

Fig. 7. Electrochemical performance and stability of tubular YSZ/Cu alloy-supported cell with infiltrated LSM cathode and brazed seal. All data obtained at 700 °C with air and 97% H_2/3% H_2O fuel. (a) Full cell AC impedance before and after ceria infiltration into anode, and after 113 h operation at 100 mA cm^{-2}, and (b) constant current conditioning at 100 mA cm^{-2}.

ment in the electrode polarization is observed. The cell was then operated for more than 100 h, as shown in Fig. 7b. Roughly linear degradation was observed during this period of constant-current operation. Fig. 7a shows AC impedance for the cell after operation. Note that the high-frequency portion has not changed, indicating conductivity in the LSM and Cu alloy phases is stable. The electrode impedance increased, approaching the shape of the impedance plot before ceria infiltration. Furthermore, the feature size of the infiltrated ceria is an order of magnitude smaller than that of the YSZ–Cu alloy backbone. Therefore we suspect that cell degradation was primarily due to evolution of the infiltrated ceria catalyst (i.e. coarsening or dewetting), and that the YSZ–Cu alloy cermet is in fact stable. Degradation of the infiltrated LSM cathode can be ruled out as a significant contributor to total cell degradation by comparison to previous work in which cells with identical cathode design displayed better stability than the cell tested here [12,14]. Modifications to the infiltrated catalyst, such as doping the ceria or choosing a different composition, are expected to improve the stability of this electrode design. It would also be feasible to add catalyst to the YSZ–Cu alloy mixture before sintering.

4. Conclusions

We have prepared YSZ–Cu alloy cermets by firing in reducing atmosphere in the temperature range 1100–1300 °C. After sintering at 1300 °C, the Cu phase wets the YSZ and forms a well-connected network that imparts high electronic conductivity to the cermet. Anode-supported cells were fabricated by cosintering YSZ–Cu alloy cermet anode and thin YSZ film electrolyte. Operation of these cells in the 700–800 °C range for over 100 h show that YSZ–Cu alloy cermet fabricated in this manner is a promising alternative anode system to the traditional Ni–YSZ. Future work should focus on improving the performance and stability of the catalyst in the anode composite.

Acknowledgements

The authors gratefully acknowledge the assistance of Tal Sholklapper for providing FIB cross section images and James Wu for vacuum brazing. This work was supported by the U.S. Department of Energy under Contract No. DE-AC02-05CH11231.

References

[1] R.J. Gorte, J.M. Vohs, Curr. Opin. Colloid Interf. Sci. 14 (2009) 236–244.
[2] A. Hornes, D. Gammara, G. Munuera, J.C. Conesa, A. Martinez-Arias, J. Power Sources 169 (2007) 9–16.
[3] USGS: Metal Prices in the United States Through 1998, http://minerals.usgs.gov/minerals/pubs/metal_prices/.
[4] S. Park, R.J. Gorte, J.M. Vohs, J. Electrochem. Soc. 148 (2001) A443–A447.
[5] M.D. Gross, J.M. Vohs, R.J. Gorte, J. Mater. Chem. 17 (2007) 3071–3077.
[6] J. Ding, N. Zhao, C. Shi, X. Du, J. Li, J. Alloys Compd. 425 (1–2) (2006) 390–394.
[7] N. Iwamoto, H. Yokoo, Eng. Fract. Mech. 40 (1991) 931–940.
[8] K. Nakashima, H. Matsumoto, K. Mori, Acta Mater. 48 (2000) 4677–4681.
[9] M.C. Tucker, C.P. Jacobson, L.C. DeJonghe, S.J. Visco, J. Power Sources 160 (2) (2006) 1049–1057.
[10] M.C. Tucker, G.Y. Lau, C.P. Jacobson, L.C. DeJonghe, S.J. Visco, J. Power Sources 171 (2007) 477–482.
[11] A.N. Nesmeyanov, in: J.I. Carasso (trans.), Vapour Pressure of the Elements Academic Press, New York, 1963.
[12] M.C. Tucker, G.Y. Lau, C.P. Jacobson, L.C. DeJonghe, S.J. Visco, J. Power Sources 175 (2008) 447–451.
[13] H. Kurokawa, T.Z. Sholklapper, C.P. Jacobson, L.C. De Jonghe, S.J. Visco, Electrochem. Solid-State Lett. 10 (9) (2007) B135–B138.
[14] M.C. Tucker, T.Z. Sholklapper, G.Y. Lau, L.C. DeJonghe, S.J. Visco, ECS Trans. 25 (2) (2009) 673–680.